NJC

PAPER

View Article Online
View Journal | View Issue

Cite this: *New J. Chem.*, 2016, 40, 7373

Structure–function relationships in single molecule rectification by *N*-phenylbenzamide derivatives†

Christopher Koenigsmann,‡[ab] Wendu Ding,‡[ac] Matthieu Koepf,[a] Arunabh Batra,[d] Latha Venkataraman,*[d] Christian F. A. Negre,*[ae] Gary W. Brudvig,*[ac] Robert H. Crabtree,*[ac] Victor S. Batista*[ac] and Charles A. Schmuttenmaer*[ac]

Received (in Montpellier, France) 17th March 2016,
Accepted 24th June 2016

DOI: 10.1039/c6nj00870d

www.rsc.org/njc

We examine structure–function relationships in a series of *N*-phenylbenzamide (NPBA) derivatives by using computational modeling to identify molecular structures that exhibit both rectification and good conductance together with experimental studies of bias-dependent single molecule conductance and rectification behavior using the scanning tunneling microscopy break-junction technique. From a large number of computationally screened molecular diode structures, we have identified NPBA as a promising candidate, relative to the other structures that were screened. We demonstrate experimentally that conductance and rectification are both enhanced by functionalization of the NPBA 4-carboxamido-aniline moiety with electron donating methoxy groups, and are strongly correlated with the energy of the conducting frontier orbital relative to the Fermi level of the gold leads used in break-junction experiments.

Introduction

According to a recent review,[1] unimolecular electronics (UME) have remained in a state of constant "adolescence" since the formal establishment of the field by Aviram and Ratner in 1974.[2] It is partially attributed to the fact that, despite a considerable number of publications, single molecules have yet to prove practical replacements for silicon-based electronic devices, largely because of the difficulties associated with reliably integrating single molecules into complex circuits.[3] As such, a variety of new directions have been proposed for the development of unimolecular rectifiers. For example, recent work has focused on developing and incorporating UMEs with the goal of regulating the directionality of charge separation and current flow through integrated molecular assemblies.[4–7]

Unimolecular devices capable of rectifying current—molecular diodes—could be used as a principal component in regulating charge separation and recombination at the dye-semiconductor interface in dye-sensitized photoelectrochemical cells (DSPCs).[4,7,8] Such diodes have to meet three essential requirements: (1) being relatively small in size (~1 nm), for easy integration into the dyes and to avoid interfering with the electronic structure of the dye, (2) able to respond to a very small applied bias,[4] and (3) exhibiting a large conductance at 0 V bias so that it does not affect the rate and efficiency of the initial injection.[6] Guided by these three requirements, we performed an extensive computational screening of a portfolio of promising structures for molecular rectification, which highlighted several promising candidates based on *N*-phenylbenzamide derivatives.[7]

Many designs of molecular diodes have been proposed and studied.[1] Many of these designs are similar to those proposed by Aviram and Ratner, and are based on donor-bridge-acceptor assemblies.[2,9–14] Other designs include fully conjugated systems with substitutions on the core of the molecule,[15] dipyrimidinyl-diphenyl derivatives,[16,17] π-stacked donor–acceptor cyclophane assemblies,[18] asymmetrical anchored molecules,[19–25] and systems with asymmetrically modified electrodes.[26–29] Recently, design schemes based on a single asymmetric frontier orbital have been proposed.[4,5,7,30] Even though many molecular rectifier designs show high rectification (RR > 1000), most of them are too complex to be integrated into molecular assemblies for devices such as DSPCs.

[a] *Yale Energy Sciences Institute, Yale University, P.O. Box 27394, West Haven, CT 06516-7394, USA*
[b] *Department of Chemistry, Fordham University, 441 East Fordham Road, Bronx, NY 10458, USA*
[c] *Department of Chemistry, Yale University, P.O. Box 208107, New Haven, CT 06520-8107, USA. E-mail: gary.brudvig@yale.edu, robert.crabtree@yale.edu, victor.batista@yale.edu, charles.schmuttenmaer@yale.edu*
[d] *Department of Applied Physics and Applied Mathematics, Columbia University, New York, NY 10027, USA. E-mail: lv2117@columbia.edu*
[e] *Theoretical Division, Los Alamos National Laboratory, P.O. Box 1663, Los Alamos, New Mexico, 87545, USA. E-mail: cnegre@lanl.gov*

† Electronic supplementary information (ESI) available: Synthetic procedures for $\mathbf{R1_A}$, $\mathbf{R2_A}$, $\mathbf{R3_A}$, and $\mathbf{R4_A}$ and additional details regarding the computational methods. See DOI: 10.1039/c6nj00870d

‡ These authors contributed equally to this work.

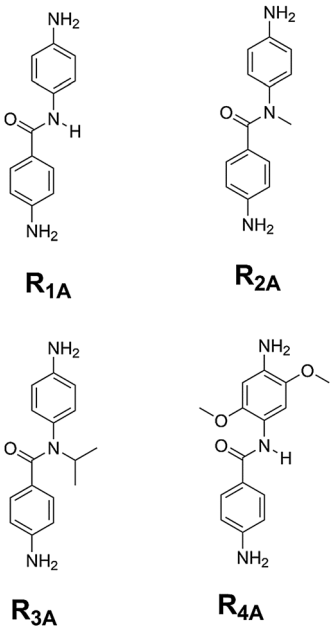

Scheme 1 Structures of our as synthesized NPBA derivatives.

Other observations of high rectifications were achieved with systems using different electrode materials or different terminal groups on either side of the junction. As pointed out by previous studies,[19,24,25,30,31] molecular rectifiers with asymmetric contacts or terminal groups can induce extrinsic rectification, which is independent of the properties of the molecules themselves. In order to meet the third requirement, it is important to consider the 'orbital rule' described by Yoshisawa and co-workers in the case of fully conjugated molecular systems.[32] This would determine the best spatial location of the anchoring groups on the molecule to avoid undesirable dephasing effects between the frontier orbital and ensure a high conductance at 0 V.

Here, we focus on the *N*-phenylbenzamide (NPBA) structure (Scheme 1, molecule $\mathbf{R1_A}$) and derivatives which are predicted to have both high conductance and rectification. The NPBA structure has several advantages in the context of molecular rectifiers, including its ease of synthesis and stability, that it can be modified with a variety of anchoring groups, and that it can be functionalized on the amide or phenyl groups to produce an extensive range of derivatives with tunable electron-transport properties.

We have synthesized four molecular rectifiers based on NPBA (Scheme 1) to explore the fundamental structure–property relationship influencing the transport properties of NPBA derivatives. Our selection of the parent NPBA molecule ($\mathbf{R1_A}$) is guided by the results of a recent computational study performed by our group, which revealed that both the conductance and rectification of NPBA derivatives are strongly correlated with the energy of the conducting frontier orbital relative to the Fermi level (E_F) of the gold leads used in break junction experiments.[7] We have synthesized two NPBA derivatives with *N*-methyl ($\mathbf{R2_A}$) and *N*-isopropyl ($\mathbf{R3_A}$) alkyl functionalities on the parent NPBA molecule. In addition, we have synthesized a NPBA derivative bearing electron donating methoxy groups on the aniline moiety ($\mathbf{R4_A}$).

Based on our computational predictions, these chemical modifications were expected to lead to changes in both the conductance and rectification properties, which we explore experimentally here. Several experimental techniques have been established to measure conductance and rectification by individual molecules, including measurements on molecules bridging electrical contacts prepared by patterned lithography,[33,34] between stretched micro-wires,[35,36] and in between the gold tip and substrate of a scanning tunneling (STM), or an atomic force (AFM) microscope.[37–41] All of these experimental methods have demonstrated that single molecules can indeed function as diodes. In this work, the current–voltage (*I–V*) characteristics of these molecules were examined by the scanning tunneling microscopy break-junction (STM-BJ) technique,[41] which probes the bias-dependent conductance of molecules bound between the gold tip and substrate of a scanning tunneling microscope.[39–41] Histograms of *I–V* curves were determined from thousands of break-junction measurements, and the results were correlated with the trends predicted by computational screening.[5]

It is important to note that the STM-BJ technique measures the *I–V* characteristics of a single molecule and is inherently different from techniques that measure the *I–V* characteristics of contacts made with molecular monolayers where many molecules are probed in a given measurement. To date, the highest rectification ratios (RR) measured by the STM-BJ technique is $\sim$200 for molecules linked to gold electrodes with asymmetric anchoring groups in ionic solutions.[42] On the other hand, measurement of *I–V* characteristics from molecular monolayers results in much higher RRs that can range up to several thousand.[1,43] Although higher RRs are measured from molecular monolayers, single molecule techniques reduce the effects of intermolecular interactions and molecular packing on the observed *I–V* characteristics.[40] Only single molecules, not monolayers, can meet the needs of molecular electronics.

Results and discussion

The series of NPBA rectifiers shown in Scheme 1 were synthesized *via* peptide coupling reactions, which enabled the parent NPBA molecule to be derivatized with alkyl groups on the amide group or electron donating groups on the aniline moiety. We expect that these chemical modifications will lead to changes in both the conductance and rectification properties, based on computational results. Fig. 1 shows the experimental histograms of molecular conductance for $\mathbf{R1_A}$, $\mathbf{R2_A}$, and $\mathbf{R4_A}$. The average conductance values measured experimentally and the calculated values are summarized in Table 1. We find that $\mathbf{R4_A}$ has the highest conductance (2.7×10^{-4} G_0) while $\mathbf{R2_A}$ (9.0×10^{-5} G_0) has the lowest conductance and is three-fold lower than that of $\mathbf{R1_A}$ (1.7×10^{-4} G_0). Based on DFT calculations, the decreased conductance of $\mathbf{R2_A}$ is attributed to the larger dihedral angle between the carbonyl group and the adjacent phenyl ring due to the steric effect of the *N*-methyl group which increases the dihedral angle from 24° in $\mathbf{R1_A}$ to 40° in $\mathbf{R2_A}$. These results are consistent with recent studies of other systems (*e.g.*, biphenyls)

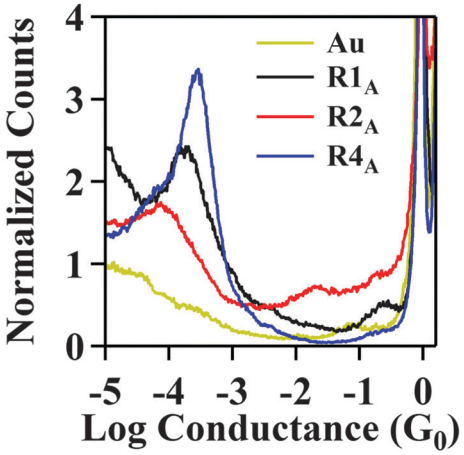

Fig. 1 Normalized, log-binned conductance histograms for $\mathbf{R1_A}$, $\mathbf{R2_A}$, and $\mathbf{R4_A}$ obtained from 5000 individual conductance traces collected at a bias of 100 mV. Au histogram generated from 1000 traces is also shown.

Table 1 Measured and calculated values of conductance (G) and rectification ratio (RR) for molecules $\mathbf{R1_A}$, $\mathbf{R2_A}$, and $\mathbf{R4_A}$

	Measured		Calculated	
Molecules	G (G_0)	RR	G (G_0)	RR
$\mathbf{R1_A}$	1.7×10^{-4}	1.3	2.6×10^{-4}	1.4
$\mathbf{R2_A}$	9.0×10^{-5}	1.3	2.2×10^{-5}	1.2
$\mathbf{R4_A}$	2.7×10^{-4}	1.5	2.9×10^{-4}	2.2

showing that conductance depends strongly on the degree of conjugation.[5,44,45] In our case, the larger dihedral angle in $\mathbf{R2_A}$ effectively breaks the conjugation and reduces the transmission probability relative to $\mathbf{R1_A}$.

The *N*-isopropyl molecule $\mathbf{R3_A}$ was successfully synthesized, but did not result in well-defined conductance plateaus in the STM-BJ measurements. Although the conductance and *I*–*V* characteristics of this molecule could not be determined, the lack of a well-defined conductance plateau has been noted previously and suggests that the binding between the target molecule and the leads is not sufficiently strong to form a stable, reproducible junction. In our case, this finding suggests that the functionalization of the amide group with *N*-alkyl groups changes the structure of the NPBA molecule more profoundly than simply changing the dihedral angle. In fact, prior studies have shown that the bent (*E*) configuration of the amide becomes more energetically favorable relative to the linear configuration (*Z*) when the amide is functionalized with alkyl group, thus hindering junction formation.[46–48]

To further investigate this, we performed DFT calculations (details in ESI†) to determine the structure of our series of molecules in the gas phase and in solution using the SMD solvation model (Density-based Solvation Model). Tetrachloroethene (or perchloroethylene, PCE) was substituted for 1,2,4-trichlorobenzene (TCB) during the solution phase calculations since TCB is not included in Gaussian 09. PCE and TCB are similar in regard to their high chlorine content and unsaturation, and also have similar dielectric constants (ε = 2.27 for PCE compared to ε = 2.24 for TCB). The free energy changes, between the bent and linear configurations of each molecule, are given in Table 2. The calculations reveal that the bent configuration is energetically favored relative to the linear configuration in the *N*-alkyl functionalized $\mathbf{R2_A}$ and $\mathbf{R3_A}$ molecules, whereas the linear configuration is favored in the unsubstituted $\mathbf{R1_A}$ and $\mathbf{R4_A}$ molecules.

Table 2 Free energy change (in kcal mol^{-1}) for bent conformer relative to linear conformer of each molecule. Solvent used for solution phase calculation is tetrachloroethene

Molecule	Gas phase	Solution phase
$\mathbf{R1_A}$	3.55	4.15
$\mathbf{R2_A}$	−3.31	−1.84
$\mathbf{R3_A}$	−7.13	−5.19
$\mathbf{R4_A}$	5.95	5.47

In STM-BJ experiments, a linear configuration (Fig. 2) is desired since the amine anchoring groups are then suitably oriented for optimal binding to the Au-leads. In the case of $\mathbf{R2_A}$, we were able to form a sufficient number of stable junctions to measure the conductance and *I*–*V* characteristics, despite the fact that the bent configuration is energetically favored.[49] Considering the Boltzmann distribution and energy difference between the linear and bent configurations, roughly 4% of $\mathbf{R2_A}$ molecules are in their linear configuration in solution at room temperature. In addition, the mechanical force imparted by the gold tip pulling away from the surface may also increase the probability of stable junction formation when the energy difference between the bent and linear configuration is relatively small, as is the case with $\mathbf{R2_A}$. On the other hand, the energy difference between the bent and linear configuration is much larger in $\mathbf{R3_A}$, and only 0.016% of them will be in the linear configuration. We believe this leads to a low yield of stable junctions and is consistent with the experimental results. This finding highlights the importance of investigating not only the electronic properties of the molecule within a junction but also the structural properties of the molecule in solution.

In addition to examining the effect of functionalizing the amide with *N*-alkyl groups, we have also introduced electron-donating –OMe groups into the 4-amino-aniline fragment of the molecule, as seen in structure $\mathbf{R4_A}$. This has shown promising enhancements in both conductance and rectification. In fact, we find that the conductance of $\mathbf{R4_A}$ (2.9×10^{-4} G_0) is nearly two-fold higher than the conductance measured for $\mathbf{R1_A}$. Since $\mathbf{R4_A}$ has a similar twist angle in the amide bridge compared to $\mathbf{R1_A}$, the increase in conductance is not due to the relative degree of conjugation, as was the case with the alkyl-functionalized NPBA derivatives. Rather, the increase in conductance is attributed to a shift in the HOMO energy associated with the peak in the transmission function, as shown in Fig. 3A. Electron-donating groups on aromatic rings generally increase the energy of the HOMO. Hence, substitution with –OMe shifts the transport channel of $\mathbf{R4_A}$ (*i.e.*, the HOMO) closest to the E_F by approximately 0.5 eV toward E_F when compared to $\mathbf{R1_A}$ and $\mathbf{R2_A}$. Therefore, the transmission for $\mathbf{R4_A}$ at E_F is higher than for $\mathbf{R1_A}$, which is fully consistent with the higher value of conductance measured.

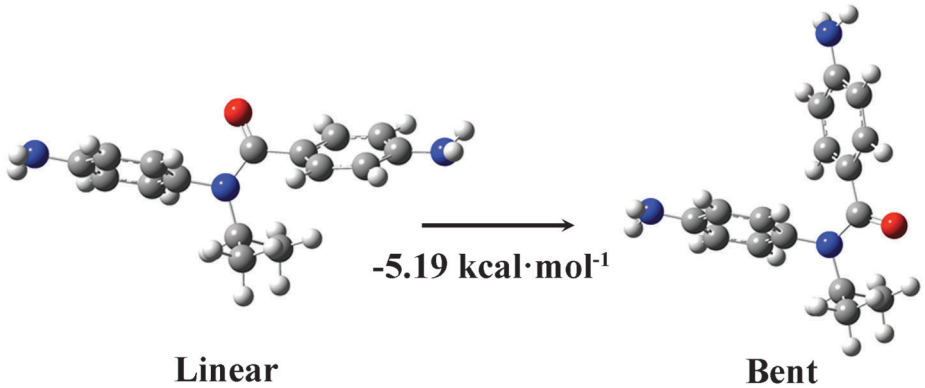

Fig. 2 The linear and bent configurations of molecule **R3$_A$**. The bent structure is calculated to be 5.19 kcal mol^{-1} more stable than the linear structure in tetrachloroethene.

Fig. 3B shows the average *I–V* curves measured for molecules **R1$_A$**, **R2$_A$**, and **R4$_A$** determined from over 2000 measurements of individual junctions obtained following methods detailed previously.[19] The magnitude of current rectification is quantified by the rectification ratio (RR = I^+/I^-) of forward (I^+) and reverse (I^-) currents obtained by applying a given bias potential, in the forward and reverse directions, respectively. The rectification ratios (Table 1) for **R1$_A$**, **R2$_A$**, and **R4$_A$** are 1.3, 1.3, and 1.5, respectively at 0.8 V. These RR values are above the baseline of 1.2 measured for symmetrical non-rectifying molecules (see Experimental methods section) and are comparable to those obtained in a prior report (~1.5 at 0.85 V) for asymmetrically coupled stilbene.[19] Although the values are lower than those recently achieved by this technique,[42] our focus here is on the trend in RR. We find that the measured trends are consistent with the trends observed by computational screening of NPBA analogs (Table 1).[7]

The RRs correlate with the energy of the transmission state corresponding to the HOMO, relative to the E_F of the extended system (including the molecule and the gold leads). This effect, previously referred to as the "E_F proximity" effect, suggests that there is a strong correlation between rectification and the energy of the transmission state relative to E_F, provided the conducting orbital (HOMO in this case) has an asymmetrical distribution of the electron density with respect to the junction.[7,30] In this case, rectification was predicted to increase as the energy of the transmission state under zero-bias approaches that of E_F. Since the rectification is caused by the asymmetrical energy shifting of the conducting HOMO under positive and negative biases, the degree of rectification under a certain bias is determined by the shifting of the HOMO in and out of the integration window, which is centered at the Fermi level. Therefore, the initial energy position of the HOMO is crucial to the impact of its shifting on the amount of the state inside the integration window: the closer the HOMO to E_F, the larger and the earlier the impact it would have.

To isolate this "E_F proximity" effect, we have minimized the effects of differences in coupling between the molecule and the lead by synthesizing molecules all with the same anchoring group, and by using gold leads on both sides of the molecule. Our experimental results demonstrate that significant changes in both conductance and rectification can be achieved by tuning both the conjugation of the NPBA molecule with alkyl

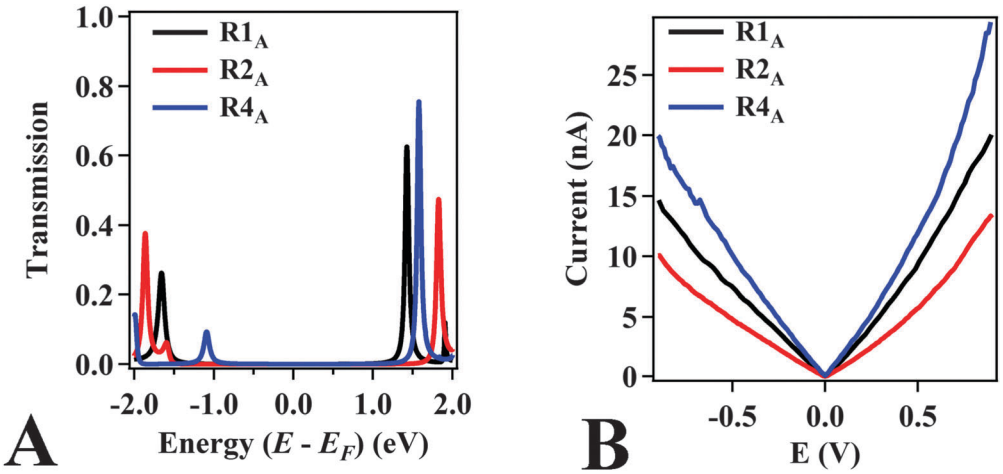

Fig. 3 The calculated transmission function (A) and the statistically most probable *I–V* curves (B) determined by the STM-BJ technique for molecules **R1$_A$**, **R2$_A$**, and **R4$_A$**. Note: the absolute value of the current is plotted.

functional groups and the energy of the HOMO level relative to E_F by adding electron donating groups to the aniline moiety.

Conclusions

Guided by computational screening, we have synthesized a series of *N*-phenylbenzamide derivatives, and characterized their conductance and rectification properties as a function of molecular structure using the scanning tunneling microscopy break junction technique. We find that rectification is increased when the *N*-phenylbenzamide backbone is functionalized with the electron-donating methoxy groups on the 4-amino-aniline fragment. Electron-donating groups raise the energy of the HOMO, which is the state that dominates conductance since it is closest to the Fermi level. The resulting proximity amplifies rectification, suggesting a simple yet robust design principle for the rational development of molecular rectifiers. Work in progress involves using these design principles to explore derivatization of *N*-phenylbenzamide with other functional groups in order to further increase molecular rectification.

Experimental methods

Details regarding the synthesis and characterization of molecules $\mathbf{R1_A}$, $\mathbf{R2_A}$, $\mathbf{R3_A}$, and $\mathbf{R4_A}$ and details of our computational methods can found in the ESI.†

Molecular conductance and *I–V* characteristics were measured by using an STM in the break-junction mode. The break-junction technique involves forming and breaking gold point contacts in a solution of the target molecules. Initially, a freshly cut gold wire (0.25 mm diameter, 99.999%, Alfa Aesar) and a mica disk coated with 100 nm of gold (99.999%, Alfa Aesar) were employed as the STM tip and substrate, respectively. The gold-coated substrate was pre-treated in a UV-ozone etcher to remove residual organic impurities immediately before performing STM experiments. The STM-BJ measurements were performed under ambient, room temperature conditions. Initially, ~1000 conductance traces were collected with the pristine gold tip and substrate in order to verify that the tip and substrate were free of contaminants.

The conductance and *I–V* characteristics of the single-molecule contacts were measured in break junctions formed in the presence of a dilute solution of the target molecule (1–10 mM) dissolved in 1,2,4-trichlorobenzene (99%, Sigma Aldrich). The tip was brought into contact with the surface of the substrate until the conductance was greater than 5 G_0 (1 G_0 = 77.5 μs). The tip was subsequently withdrawn at a rate of 15 nm s^{-1} for a period of 125 ms and held for a period of 150 ms, while a triangular voltage ramp was applied between +1 V and −1 V. Finally, the tip was withdrawn at 15 nm s^{-1} for a period of 75 ms to break the junction before repeating the process for a total of ~50 000 individual traces. The collected traces were analyzed to select traces that maintained a molecular junction during the entire *I–V* ramp (1–10% of all measured traces). A data selection and sorting process, described in detail elsewhere, was then employed to generate histograms of the *I–V* curves to obtain the average *I–V* curve.[19]

Acknowledgements

This work was funded by the U.S. Department of Energy, Office of Science, Office of Basic Energy Sciences under Award Number DE-FG02-07ER15909 and a generous gift from the TomKat Charitable Trust. Computational methods development (V. S. B.) were supported as part of the Argonne-Northwestern Solar Energy Research (ANSER) Center, an Energy Frontier Research Center funded by the U.S. Department of Energy, Office of Science, Office of Basic Energy Sciences under award no. DE-SC0001059, using computational resources from NERSC and from the Yale University Faculty of Arts and Sciences High Performance Computing Center partially, funded by the National Science Foundation grant CNS 08-21132. L. V. thanks the Packard Foundation for support. A. B. was supported by the NSF GRFP Grant No. DGE-07-07425. We also acknowledge the Yale West Campus Analytical Core for providing access to NMR spectrometers, and thank Dr Terence Wu for assistance with the high-resolution mass spectrometry.

Notes and references

1 R. M. Metzger, *Chem. Rev.*, 2015, **115**, 5056–5115.
2 A. Aviram and M. A. Ratner, *Chem. Phys. Lett.*, 1974, **29**, 277–283.
3 M. Ratner, *Nat. Nanotechnol.*, 2013, **8**, 385–389.
4 W. Ding, C. F. A. Negre, J. L. Palma, A. C. Durrell, L. J. Allen, K. J. Young, R. L. Milot, C. A. Schmuttenmaer, G. W. Brudvig, R. H. Crabtree and V. S. Batista, *ChemPhysChem*, 2014, **15**, 1138–1147.
5 W. Ding, C. F. A. Negre, L. Vogt and V. S. Batista, *J. Phys. Chem. C*, 2014, **118**, 8316–8321.
6 C. F. A. Negre, R. L. Milot, L. A. Martini, W. Ding, R. H. Crabtree, C. A. Schmuttenmaer and V. S. Batista, *J. Phys. Chem. C*, 2013, **117**, 24462–24470.
7 W. Ding, M. Koepf, C. Koenigsmann, A. Batra, L. Venkataraman, C. F. A. Negre, G. W. Brudvig, R. H. Crabtree, C. A. Schmuttenmaer and V. S. Batista, *J. Chem. Theory Comput.*, 2015, **11**, 5888–5896.
8 A. Monti, C. F. A. Negre, V. S. Batista, L. G. C. Rego, H. J. M. de Groot and F. Buda, *J. Phys. Chem. Lett.*, 2015, **6**, 2393–2398.
9 R. M. Metzger, *Mater. Sci. Eng., C*, 1995, **3**, 277–285.
10 A. S. Martin and J. R. Sambles, *Nanotechnology*, 1996, **7**, 401.
11 W. J. Shumate, D. L. Mattern, A. Jaiswal, D. A. Dixon, T. R. White, J. Burgess, A. Honciuc and R. M. Metzger, *J. Phys. Chem. B*, 2006, **110**, 11146–11159.
12 A. Honciuc, R. M. Metzger, A. Gong and C. W. Spangler, *J. Am. Chem. Soc.*, 2007, **129**, 8310–8319.
13 R. M. Metzger, B. Chen, U. Höpfner, M. V. Lakshmikantham, D. Vuillaume, T. Kawai, X. Wu, H. Tachibana, T. V. Hughes, H. Sakurai, J. W. Baldwin, C. Hosch, M. P. Cava, L. Brehmer and G. J. Ashwell, *J. Am. Chem. Soc.*, 1997, **119**, 10455–10466.
14 S. K. Yee, J. Sun, P. Darancet, T. D. Tilley, A. Majumdar, J. B. Neaton and R. A. Segalman, *ACS Nano*, 2011, **5**, 9256–9263.

15 J. Reichert, R. Ochs, D. Beckmann, H. B. Weber, M. Mayor and H. v. Löhneysen, *Phys. Rev. Lett.*, 2002, **88**, 176804.
16 I. Diez-Perez, Z. Li, J. Hihath, J. Li, C. Zhang, X. Yang, L. Zang, Y. Dai, X. Feng, K. Muellen and N. Tao, *Nat. Commun.*, 2010, **1**, 31.
17 J. Hihath, C. Bruot, H. Nakamura, Y. Asai, I. Díez-Pérez, Y. Lee, L. Yu and N. Tao, *ACS Nano*, 2011, **5**, 8331–8339.
18 Y. Tsuji and K. Yoshizawa, *J. Phys. Chem. C*, 2012, **116**, 26625–26635.
19 A. Batra, P. Darancet, Q. Chen, J. S. Meisner, J. R. Widawsky, J. B. Neaton, C. Nuckolls and L. Venkataraman, *Nano Lett.*, 2013, **13**, 6233–6237.
20 C. Van Dyck and M. A. Ratner, *Nano Lett.*, 2015, **15**, 1577–1584.
21 J. Ma, C.-L. Yang, M.-S. Wang and X.-G. Ma, *RSC Adv.*, 2015, **5**, 10675–10679.
22 K. Garg, C. Majumder, S. K. Nayak, D. K. Aswal, S. K. Gupta and S. Chattopadhyay, *Phys. Chem. Chem. Phys.*, 2015, **17**, 1891–1899.
23 H. J. Yoon, K.-C. Liao, M. R. Lockett, S. W. Kwok, M. Baghbanzadeh and G. M. Whitesides, *J. Am. Chem. Soc.*, 2014, **136**, 17155–17162.
24 K. Wang, J. Zhou, J. M. Hamill and B. Xu, *J. Chem. Phys.*, 2014, **141**, 054712.
25 A. Batra, J. S. Meisner, P. Darancet, Q. Chen, M. L. Steigerwald, C. Nuckolls and L. Venkataraman, *Faraday Discuss.*, 2014, **174**, 79–89.
26 J. Li, Z. H. Zhang, M. Qiu, C. Yuan, X. Q. Deng, Z. Q. Fan, G. P. Tang and B. Liang, *Carbon*, 2014, **80**, 575–582.
27 B. Capozzi, J. Xia, O. Adak, E. J. Dell, Z.-F. Liu, J. C. Taylor, J. B. Neaton, L. M. Campos and L. Venkataraman, *Nat. Nanotechnol.*, 2015, **10**, 522–527.
28 Y. Song, Z. Xie, Y. Ma, Z.-l. Li and C.-K. Wang, *J. Phys. Chem. C*, 2014, **118**, 18713–18720.
29 T. Kim, Z.-F. Liu, C. Lee, J. B. Neaton and L. Venkataraman, *Proc. Natl. Acad. Sci. U. S. A.*, 2014, **111**, 10928–10932.
30 W. Ding, C. F. A. Negre, L. Vogt and V. S. Batista, *J. Chem. Theory Comput.*, 2014, **10**, 3393–3400.
31 J. B. Pan, Z. H. Zhang, K. H. Ding, X. Q. Deng and C. Guo, *Appl. Phys. Lett.*, 2011, **98**, 092102.
32 K. Yoshizawa, *Acc. Chem. Res.*, 2012, **45**, 1612–1621.
33 J. Park, A. N. Pasupathy, J. I. Goldsmith, C. Chang, Y. Yaish, J. R. Petta, M. Rinkoski, J. P. Sethna, H. D. Abruna, P. L. McEuen and D. C. Ralph, *Nature*, 2002, **417**, 722–725.
34 W. Liang, M. P. Shores, M. Bockrath, J. R. Long and H. Park, *Nature*, 2002, **417**, 725–729.
35 M. A. Reed, C. Zhou, C. J. Muller, T. P. Burgin and J. M. Tour, *Science*, 1997, **278**, 252–254.
36 J. C. Cuevas and E. Scheer, *Molecular Electronics: An Introduction to Theory and Experiment*, World Scientific Publishing Company Pte Limited, 2010.
37 X. Xiao, B. Xu and N. J. Tao, *Nano Lett.*, 2004, **4**, 267–271.
38 L. Venkataraman, J. E. Klare, I. W. Tam, C. Nuckolls, M. S. Hybertsen and M. L. Steigerwald, *Nano Lett.*, 2006, **6**, 458–462.
39 V. Kaliginedi, P. Moreno-García, H. Valkenier, W. Hong, V. M. García-Suárez, P. Buiter, J. L. H. Otten, J. C. Hummelen, C. J. Lambert and T. Wandlowski, *J. Am. Chem. Soc.*, 2012, **134**, 5262–5275.
40 S. V. Aradhya and L. Venkataraman, *Nat. Nanotechnol.*, 2013, **8**, 399–410.
41 B. Xu and N. J. Tao, *Science*, 2003, **301**, 1221–1223.
42 B. Capozzi, J. Xia, O. Adak, E. J. Dell, Z.-F. Liu, J. C. Taylor, J. B. Neaton, L. M. Campos and L. Venkataraman, *Nat. Nanotechnol.*, 2015, **10**, 522–527.
43 R. M. Metzger, *Synth. Met.*, 2009, **159**, 2277–2281.
44 L. Venkataraman, J. E. Klare, C. Nuckolls, M. S. Hybertsen and M. L. Steigerwald, *Nature*, 2006, **442**, 904–907.
45 A. Mishchenko, D. Vonlanthen, V. Meded, M. Bürkle, C. Li, I. V. Pobelov, A. Bagrets, J. K. Viljas, F. Pauly, F. Evers, M. Mayor and T. Wandlowski, *Nano Lett.*, 2010, **10**, 156–163.
46 A. Itai, Y. Toriumi, N. Tomioka, H. Kagechika, I. Azumaya and K. Shudo, *Tetrahedron Lett.*, 1989, **30**, 6177–6180.
47 S. Saito, Y. Toriumi, N. Tomioka and A. Itai, *J. Org. Chem.*, 1995, **60**, 4715–4720.
48 R. Yamasaki, A. Tanatani, I. Azumaya, S. Saito, K. Yamaguchi and H. Kagechika, *Org. Lett.*, 2003, **5**, 1265–1267.
49 A. J. Bloomfield, S. Chaudhuri, B. Q. Mercado, V. S. Batista and R. H. Crabtree, *New J. Chem.*, 2016, **40**, 1974–1981.

